fortune Journals

Research Article

JOURNAL OF CANCER SCIENCE AND CLINICAL THERAPEUTICS

ISSN: 2637-5079

Astaxanthin-Mediated Returning the Aquaporin-1 to Basal Level May be an Alternative Treatment Approach in Radiotherapy-Induced Lung Injury

Akın SE[1*], Erzurumlu Y[2], Camas HE[1], Buyukbayram HI[3], Ascı H[4], Hasseyid N[4], Ozmen O[5]

Abstract

Background: Radiotherapy (12-RAD), which has an important place in cancer treatment, destroys cancer cells, but also negatively affects healthy tissues in that area. Astaxanthin (ATX) is known to have powerful antioxidant, anti-inflammatory and antiapoptotic properties. In this study, we aimed to evaluate the effects of ATX on lung injury after radiotherapy.

Methods and Results: 32 rats were divided into 4 groups as control, 12-RAD (a single dose of 10 Gy x-ray was given at a rate of 0.62 Gy/min), 12-RAD+ATX, + ATX (10mg/kg ATX was administered by oral gavage for 7 days). Twenty-four hours after the last ATX application, the lung tissues of the rats were taken for biochemical, genetic, histopathological, and immunohistochemical examinations. 12-RAD increased the oxidative stress markers TOS, OSI levels, the expression of VCAM-1, VEGF-A, which increases in inflammation, and the apoptotic marker, caspase-3. It also significantly reduced Aquaporin-1 and TAS levels. On the other hand, ATX has returned all these parameters.

Conclusion: All evidence suggests that the use of ATX may be a potential therapeutic agent against radiotherapy-induced lung injury.

Keywords: Acute lung injury; Inflammation; Aquaporin-1; Astaxanthin; Radiotherapy.

Introduction

Many years ago, Marie Curie was a pioneer in the field of radiation therapy and won the Nobel Prize for her discovery on radium. In 1895, X-rays were started to be used clinically by Wilhelm Conrad Röntgen in Germany and this situation paved the way for it to take place in cancer treatment. In the process to date, radiation therapy has become a medical discipline known for radiation oncology, where experts from many disciplines work together [1]. Radiotherapy has an important place in cancer management. Radiation therapy is given to more than half of patients with cancer either alone or in combination [2]. Unfortunately, while it destroys the cancer cells of the patients receiving this treatment, it also affects the healthy tissues of the cancerous tissue in a negative way. It causes lesions in the irradiated area and damage in that area. These lesions may progress to cause fibrosis and adhesions in different parts of the body [3]. Radiation; since it disrupts the epithelial and endothelial integrity, a series of molecular events are triggered by the cells here, the inflammation process is initiated in the lung tissue, and if this process progresses further, it can cause oxidative stress. During the radiation-induced lung stages, dose-related protein leakage into the alveolar space, alveolar septa thickening, interstitium edema, displacement of capillaries.

Affiliation:

[1]Suleyman Demirel University, Faculty of Medicine, Thoracic Surgery Department, Isparta, Turkey

[2]Suleyman Demirel University, Faculty of Pharmacy, Department of Biochemistry, Isparta, Turkey

[3]Suleyman Demirel University, Faculty of Medicine, Department of Medical Biochemistry, Isparta, Turkey

[4]Suleyman Demirel University, Faculty of Medicine, Department of Pharmacology, Isparta, Turkey

[5]Burdur Mehmet Akif Ersoy University, Faculty of Veterinary Medicine, Department of Pathology, Burdur, Turkey

***Corresponding author:**
Assist. Prof. Suleyman Emre AKIN, Suleyman Demirel University, Medical Faculty Department of Thoracic Surgery, Isparta, Turkey

Citation: Akın SE, Erzurumlu Y, Camas HE, Buyukbayram HI, Ascı H, Hasseyid N, Ozmen O. Astaxanthin-Mediated Returning the Aquaporin-1 to Basal Level May be an Alternative Treatment Approach in Radiotherapy-Induced Lung Injury. Journal of Cancer Science and Clinical Therapeutics. 8 (2024): 135-142.

Received: May 09, 2024
Accepted: May 24, 2024
Published: June 20, 2024

In this process alveolar macrophages appear and type II pneumocytes change [4]. Several molecular mechanisms that cause cellular stress control radiation-induced cell death. Cellular stress is followed by cellular aging or death, depending on the dose and irradiation protocols used [5]. The primary purpose of radiotherapy is to stop the process of cell division and induce apoptosis in cancer cells [6].

Apoptosis is a regulated, programmed kind of cell death [7]. Cancer is the discontinuous, uncontrolled, irregular growth process of cells. Cancerous cells do not respond to the death command and are the cells that manage to escape apoptosis. One of the defining features of cancer is apoptosis resistance. Breaking this cell resistance mechanism is the main goal of the therapeutic intervention. Following these interventions, the application of chemotoxic agents or high doses of radiation to overcome the apoptosis barrier in cancerous cells triggers damage mechanisms in healthy tissue. Therefore, it is necessary to consider new alternatives that maximize the apoptosis of cancerous cells and minimize damage to healthy cells [8]. One of the specific features of apoptosis is a family of enzymes called caspases (CAS). Death signals result in the activation of the cas family, which is responsible for the final stage of cell destruction. Then, apoptotic bodies are formed in the process known as efferocytosis to be engulfed by phagocytic cells [7]. As a result, the cell becomes involved in the apoptosis process. Natural substances known as carotenoids are produced by plants and some photosynthetic microorganisms. Many carotenoids directly contribute to the process of photosynthesis, while others defend the host against photooxidation and associated injury. Red carotenoid pigment astaxanthin (ATX) (3,3'-dihydroxy-β, β'-carotene-4,4'-dione), also known as xanthophyll, is well known for its potent antioxidant properties. The effects of ATX at the cellular level are associated with its antioxidant, anti-inflammatory and antiapoptotic properties. Preclinical and clinical research on the effects of ATX have risen significantly in the last few years. ATX is a potential medication for prevention for many diseases [9, 10]. In this research, we wanted to determine ATX's impact on lung damage following radiotherapy.

Materials and Methods

Design of experiment and study animals

Suleyman Demirel University's local animal ethics committee accepted the animal experiments. (Ethic No: 07.01.2021/01-05) Suleyman Demirel University's Scientific Research Projects Coordination Unit supported funding for this study under the project code TSG-2020-8134. We used 32 adult female Wistar albino rats weighing 300–350 g and kept at 21–22 °C, 60 ± 5% humidity with a 12 h light:12 h dark cycle. Rats were fed a regular commercial chow (Korkuteli Yem, Antalya, Turkey). The study groups were divided into four groups of ten each: control, 12-RAD, 12-RAD+ATX, and ATX groups.

1- Control group (n=10); On the first day of the research, all experimental animals will be given the same cage conditions without being exposed to X-rays after anesthesia with 10 mg/kg xylazine (Alfazin, Alfasan IBV, Turkey); 90 mg/kg ketamine (Alfamin, Alfasan IBV, Turkey). The gavage technique was used to apply 1 ml saline for 7 days.

2- 12-RAD group (n=10); On the first day of the research, after anesthesia of 10 mg/kg xylazine (Alfazin, Alfasan IBV, Turkey); 90 mg/kg ketamine (Alfamin, Alfasan IBV, Turkey) i.p, all experimental animals were given a single dose of 10 Gy X-ray at a rate of 0.62 Gy/min. was applied to the body (600C linear accelerator, Varian, USA). The gavage technique was used to apply 1 ml saline for 7 days.

3- 12-RAD + ATX group (n=10); On the first day of the research, all experimental animals were given 10 mg/kg xylazine (Alfazin, Alfasan IBV, Turkey) and 90 mg/kg ketamine (Alfamin, Alfasan IBV, Turkey) i.p as a single dose of 10 Gy X-ray at a rate of 0.62 Gy/min. was applied to the body (600C linear accelerator, Varian, USA), and 1 ml of 10mg/kg ATX was applied by oral gavage method for 7 days.

4- ATX group (n=10); On the first day of the research, all experimental animals were administered i.p with 10 mg/kg xylazine (Alfazin, Alfasan IBV, Turkey); 90 mg/kg ketamine (Alfamin, Alfasan IBV, Turkey) for 7 days with 1 ml 10mg/kg ATX oral gavage method. All rats were anesthetized with 8-10 mg/kg Xylazine (Alfazin, Alfasan IBV); 80-100 mg/kg Ketamine (Alfamine, Alfasan IBV) 24 hours after the last dose of medication. Blood samples were collected from the rats' inferior vena cava who underwent abdominal incision following anesthesia. Then, half of the tissues taken were wrapped with aluminum foil in a cold environment and brought to -20°C for biochemical and genetic analysis.

Histopathology analysis

Lung samples were taken and fixed in 10% formaldehyde during autopsy. After that the samples were regularly processed by an automated tissue processing equipment (Leica ASP300S, Wetzlar, Germany) and embedded in paraffin wax. A rotary microtome (Leica RM2155, LeicaMicrosystems, Wetzlar, Germany) was used to cut tissue sections at a thickness of 4 micrometers. Afterward it was stained with Hematoxylin&Eosin (HE), covered with a coverslip with a mounting medium, and viewed under light microscope.

Immunohistochemistry analysis

Lung samples by streptavidin-biotin technique cas-3 (Anti cas-3 antibody (31A1067):sc-56053) vascular cell adhesion molecule-1 (VCAM-1). 1 (Anti VCAM-1 antibody (M/K-2):sc-18864) all primary sera and secondary antibodies were purchased from Abcam (Cambridge, UK). Primary antibodies were used at 1/100 dilution for immunohistochemistry analysis. Using biotinylated secondary antibodies and streptavidin-

alkaline phosphatase conjugate, immunohistochemistry was carried out after primary antibodies were incubated for 60 min. The ready-to-use kit [EXPOSE Mouse and Rabbit Specific HRP / DAB Detection IHC kit (ab80436)] was used as the secondary antibody and 3,3-diaminobenzidine (DAB) as the chromogen for 5 minutes. The primary antiserum step was skipped for negative controls. For all examinations, blind samples were used. The percentage of cells that were positive for each marker was calculated statistically using the 100 cells counted by the Image Analyzer in 10 different fields for each region under the X40 objective. The Database Manual Cell Sens Life Science Imaging Software System used for morphometric analyses (Olympus Co., Tokyo, Japan).

Biochemical analysis

Lung tissue underwent an analysis for oxidative stress. The lung tissues were homogenized with an IKA Ultra Turrax T25 disperser (Germany) following 5 fold (w/v) dilution with phosphate-buffered saline (0,01 M, pH 7,4). Then, the samples were centrifuged (2000 rpm, 20 min, +4°C) and supernatants were acquired for biochemical assays. Tissue TAS (total antioxidant status), and TOS (total oxidant status) amounts were analyzed on an autoanalyzer (Beckman Coulter AU 5800, USA) and OSIs (oxidative stress index) were computed [11, 14]. Erel's automated colorimetric measurement technique was used to measure TAS [12]. The mechanism underlying the technique is the reduction of the blue-green colored 2,2′-azino-bis (3-ethylbenzthiazoline-6-sulfonic acid) (ABTS) radical to an achromic deprotonated ABTS. The optical density change at 660 nm reflects the sample TAS extent. The unit of the TAS concentration is given as mmol Trolox equiv/l. Lung tissue TOS extent was analyzed by a colorimetric procedure [13]. The ferrous ion-dianisidine complex is oxidized by oxidants in the sample to ferric ion. In an acidic environment, a colored compound is formed from the ferric ion and xylenol orange. The increase in the color intensity reflects the oxidant level in the sample. The results were given as μmol hydrogen peroxide equiv/l [13]. OSI was calculated by the formula: OSI = [(TOS / (TAS) × 100] [14].

Reverse transcription-polymerase chain reaction (RT-qPCR)

Total RNA was extracted from rat lung tissues by using AurumTM Total RNA mini kit (Bio-Rad Laboratories, Hercules, CA) following the manufacturer's instructions. The concentration and purity of isolated RNAs were determined by Allseng Nano 400A microvolume spectrophotometer (Allsheng, Hanngzou, China). 1 μg RNA was reverse transcribed with the iScript cDNA Synthesis kit by using oligo dT primers (Bio-Rad Laboratories, Hercules, CA). The reaction mix was incubated for 5 min at 25°C, for 20 min at 46°C, and for 1 min at 95℃. Real-time PCR amplification was performed using iTaq Universal SYBR Green Supermix (Bio-Rad Laboratories, Hercules, CA) according to the manufacturer's instructions, and a fluorescence signal was detected on a CFX Connect instrument (Bio-Rad Laboratories, Hercules, CA). Specific primers were designed to amplify VEGF-A (Forward 5'-GGAAGAGAGAGAGAGAGAGAC-3', Reverse 5'-GACTGGTCCGATGAAAGATCC-3'), Aquaporin-1 (AQP-1) (Forward 5'-CTGAGGAAAGAAGCAGCTAGAC-3', Reverse 5'-CTCATAAGCCAGGACAAGAGTG-3') and Glyceraldehyde-3-phosphate dehydrogenase (GAPDH) (Forward 5'-CAAGGTCATCCCAGAGCTGAA-3', Reverse 5'-CATGTAGGCCATGAGGTCCAC-3'). For each PCR, cDNA samples were examined in triplicates. The expression of VEGF-A and AQP-1 were detected, and GAPDH was used as a housekeeping gene for normalization. The following PCR conditions were used: denaturation at 95 °C for 10 min, followed by 40 cycles of: 10 s at 95 °C, 30 s at 60 °C. The total reaction volume was 25μl, 100ng cDNA was used as the template. Using the comparative 2ΔΔCt analysis approach, relative quantification of gene expression was carried out. All results showed in the graph with a fold change.

Statistical analysis

The biochemical scores of the groups were compared. One-way ANOVA post hoc LSD test was used. Using the SPSS 18.0 software package (SPSS Inc., Chicago, IL), statistical calculations were performed. Database Manual Cell Sens Life Science Imaging Software System (Olympus Co., Tokyo, Japan) used for morphometric analyzes. $p < 0.05$ was set as the significance value.

Results

Histopathological Lung Findings

Pathological signs weren't seen in the lung tissues of the control group during the microscopic examination. In the 12-RAD group, alveolar hemorrhage was observed in one, while congestion was observed in all animals. It was observed that the treatment groups treated with 12-RAD+ATX decreased histopathologically compared to the 12-RAD group. Pathological findings weren't observed in the groups that were administered only ATX (Figure 1).

In the control group, there was no evidence of expression with cas-3. Cas -3 positive (+) accumulation was observed in the alveoli for 12-RAD group. It was observed that cas-3 positivity decreased in the 12-RAD+ATX applied group. Expression with cas-3 was not observed in the ATX administered group (Figure 2). Expression with VCAM-1 was not observed in the control group. In the 12-RAD group, there is weak accumulation positivity around the bronchioles and on the alveolar walls. Its positivity was VCAM-1. No expression was observed in the 12-RAD+ATX administered group (Figure 3). VCAM-1 expression was not seen in the ATX group (Table 1).

Akın SE, et al., J Cancer Sci Clin Ther 2024
DOI:10.26502/jcsct.5079234

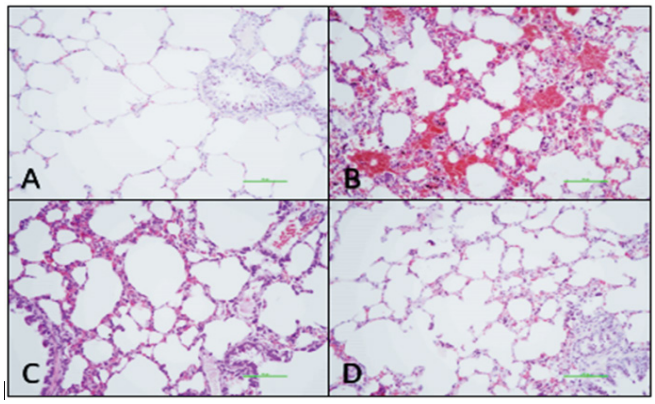

Figure 1: Representative histopathological microphotos between the groups.

(A) No expression was observed in the control group, (B) Congestion and bleeding in the alveoli were observed in the 12-RAD group (C) In the 12-RAD+ATX group, there was a decrease in the findings (D) No expression was observed in the ATX group (HE, 200X).

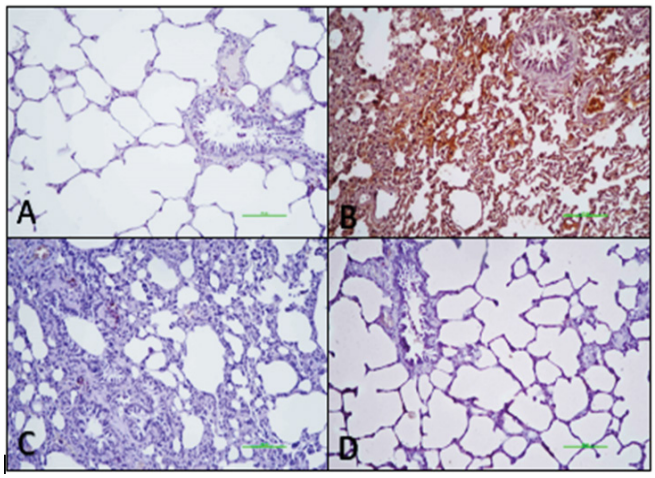

Figure 2: Cas-3 immunohistochemical finding between the groups.

(A) Cas-3 expression was not observed in the control group, (B) Cas-3 positivity in the alveolar walls of the 12-RAD group (+), (C) In the 12-RAD+ATX group, no expression was observed in the alveoli except positivity in the focal vessel wall (D) No expression was observed in Cas-3 in the ATX group (Cas-3, DAB, 200X).

TAS, TOS and OSI Results

Significant reduction in TAS level for 12-RAD group compared to the Control group (p=0.002). On the other hand, it was observed to be significantly higher in the 12-RAD+ATX group than in the 12-RAD group (p=0.019).

There was a significant increase in OSI and TOS levels in the 12-RAD group compared to the control group (p= 0.004, p <0.001 respectively). There was a significant decrease in OSI and TOS levels in the 12-RAD+ATX group compared to the 12-RAD group (p= 0.025, p< 0.001, respectively) (Figure 4).

Relative mRNA expression level of VEGF-A/AQP-1 in Lung Tissue

Relative VEGF-A mRNA levels observed significantly higher in the 12-RAD group than in the control and ATX groups (p <0.001). In 12-RAD+ATX group, mRNA expression of VEGF-A decreased compared with the 12-RAD group (not significant) (Figure 5). Also AQP-1 level was found to be significantly lower in the 12-RAD group compared to the control group (p= 0.006). A significant increase in the AQP-1 level was observed in the 12-RAD+ATX group compared to the 12-RAD group (p= 0.045) (Figure 5).

Discussion

Ionizing radiation exerts its effectiveness by seriously damaging rapidly proliferating tumor cells. Unfortunately, it also damages healthy cells in the area where the radiation is applied. Radiation damage also triggers inflammation [15]. Inflammation is a vital response. Inflammation is a comprehensive, complex physiological response process against all kinds of harmful factors that may pose a threat

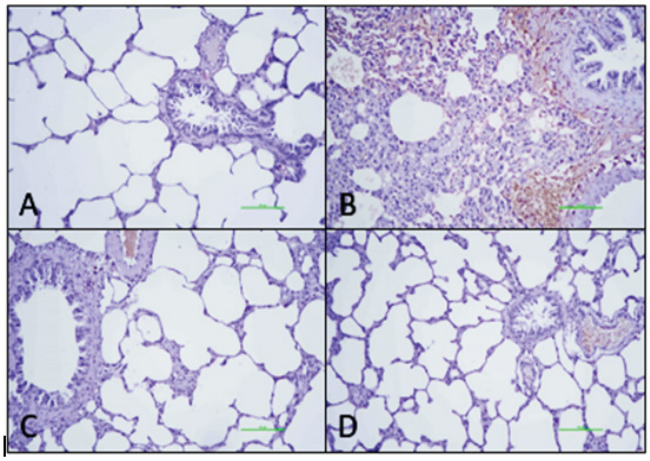

Figure 3: VCAM-1 immunohistochemical finding between the groups.

(A) No expression was observed in VCAM-1 in the control group, (B) Weak accumulation of VCAM-1 positivity around the bronchiole and alveolar walls in the 12-RAD group (+), (C) No expression was observed in the 12-RAD+ATX group (D) In the ATX group No expression was observed in VCAM-1 (VCAM-1, DAB, 200X).

Table 1: Histopathological changes in lung of the experiment groups

GROUPS	VCAM-1		Cas-3	
	Mean±SD	*p value*	*Mean±SD*	*p value*
Control	0.00 ± 0.00		0.00 ± 0.00	
12-RAD	1.25 ± 0.70[a]	a: 0.000	1.12 ± 0.83[a]	a: 0.000
12-RAD+ATX	0.25 ± 0.46[b]	b: 0.000	0.37 ± 0.51[b]	b: 0.005
ATX	0.00 ± 0.00[b]	b: 0.000	0.00 ± 0.00[b]	b: 0.000

Values were presented as means ± SD. 12-RAD: Radiation; 12-RAD+ATX: Radiation + Astaxanthin; ATX: Astaxanthin, a: Control and others; b: 12-RAD and others

Citation: Akın SE, Erzurumlu Y, Camas HE, Buyukbayram HI, Ascı H, Hasseyid N, Ozmen O. Astaxanthin-Mediated Returning the Aquaporin-1 to Basal Level May be an Alternative Treatment Approach in Radiotherapy-Induced Lung Injury. Journal of Cancer Science and Clinical Therapeutics. 8 (2024): 135-142.

Akın SE, et al., J Cancer Sci Clin Ther 2024
DOI:10.26502/jcsct.5079234

Figure 4: TAS, TOS and OSI Levels in Lung Tissue

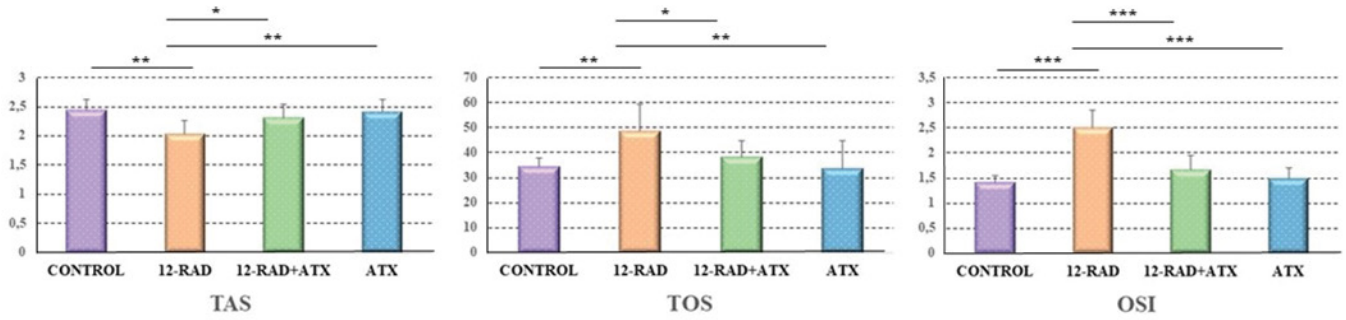

Values were presented as means ± SD. 12-RAD: Radiation; 12-RAD+ATX: Radiation + Astaxanthin; ATX: Astaxanthin; TAS: Total Antioxidant Status; TOS: Total Oxidant Status; OSI: Oxidative Stress Index *: p<0,05, **: p<0,01, ***: p<0,001

Figure 5: VEGF-A and Aquaporin-1 Levels in Lung Tissue

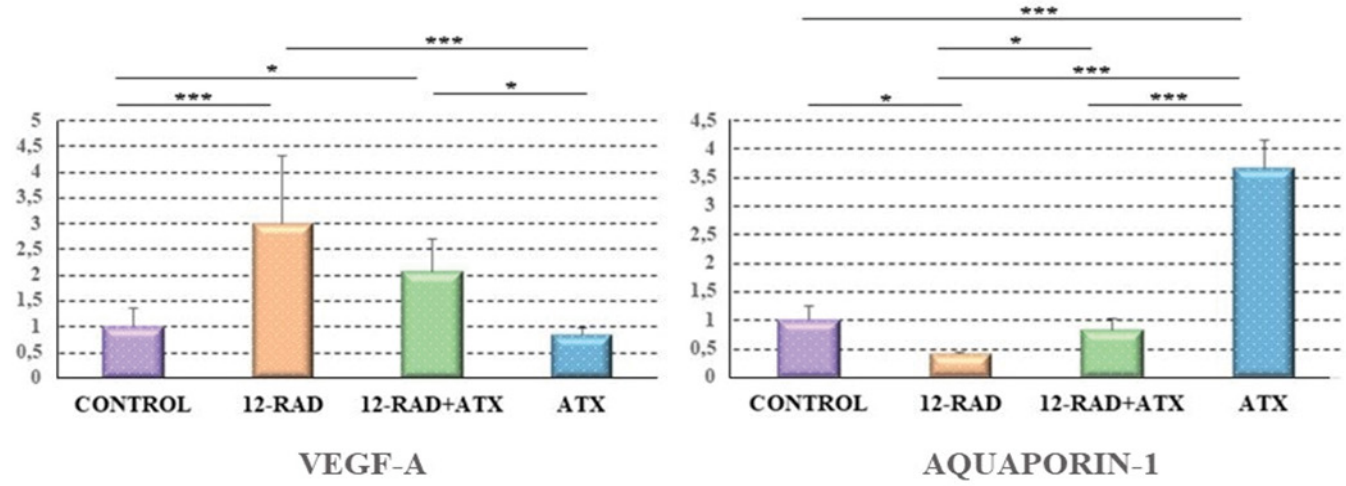

Values were presented as means ± SD. 12-RAD: Radiation; 12-RAD+ATX: Radiation + Astaxanthin; ATX: Astaxanthin;*: p<0,05, **: p<0,01, ***: p<0,001

to the organism. Inflammation basically; considering the mechanisms that occur at the cellular level, is divided into two as acute and chronic. Acute inflammation is a short process. In this process, infiltration of plasma proteins, fluids and chemotaxis of leukocytes into the extravascular space occur. Chronic inflammation occurs either through the presence of infections that cannot be resolved in endogenous defense mechanisms or through another resistance mechanism derived from host defense [16]. There are four important steps in the inflammatory response: inflammatory inducers, sensors that detect them, inflammatory mediators induced by sensors, and target tissues affected by inflammatory mediators. These chemical combinations work in several inflammatory pathways. Depending on the type of inflammatory trigger, the type of pathway induced under certain conditions varies [17]. The vascular endothelium allows the blood to flow smoothly in the lumen; and forms the interface between blood and tissues. It plays an important role in supporting the inflammatory response by first providing adhesion of circulating leukocytes to the vessel wall and then migration to the surrounding tissues. The expression of VCAM-1 is one of the initial and crucial steps in the endothelial response to inflammatory stimuli. This protein mediates the binding of leukocytes to the endothelial wall and then rolls over the endothelial surface. Tight adhesion and migration during its progression in the endothelium prepare the ground for an inflammatory response in the damaged tissue [18]. As we expected in the findings we obtained in the histopathological results, an increase in VCAM-1 levels was detected in the 12-RAD group. Considering that the increase in VCAM-1 levels is associated with inflammation, we can conclude that radiotherapy contributes to inflammation by increasing VCAM-1 levels. ATX treatment decreased the VCAM-1 levels, regressed the severity of inflammation, and regressed the damage in the lung tissue.

Alveolar damage occurs after radiotherapy secondary to inflammation. Because of the increased vascular permeability and protein exudation, this results in edema of the alveolar

Akın SE, et al., J Cancer Sci Clin Ther 2024
DOI:10.26502/jcsct.5079234

walls. Several pathological conditions (for example, respiratory distress syndrome and pulmonary edema caused of injury or infection) can seriously affect the lungs, resulting in impaired fluid transport by AQPs [19]. Small, intrinsic membrane proteins called AQPs allow water to pass more easily across cell membranes and create an intercellular channel for water to go through the epithelium [20, 21]. AQPs are present in numerous tissues, including the lungs, kidneys, and eyes, where fast water transport is critical and required. AQP-1 and AQP-5 are the two major AQPs in peripheral lung tissues [22]. AQP-1 has a significant role in water balance of the respiratory system [23]. In a study, after acute adenoviral infection, AQP1 and AQP5 levels in mouse lungs decreased. Loss of AQP1 in these mice has been shown to result in a 10-fold reduction in osmotic water transport between capillary compartments and airspace [19]. In this study, the 12-RAD group's lung tissue AQP-1 level decreased. From this point of view, radiotherapy caused serious damage by reducing AQP-1 level in the lung tissue and impairing the intercellular water transport function. This damage has been demonstrated by genetic analysis. ATX administration caused a significant increase in AQP-1 level, preventing the decrease caused by radiotherapy. It also significantly reduced the damage caused by the change in AQP-1 level. One of the most essential growth factors for controlling vascular development and angiogenesis is vascular endothelial growth factor-A (VEGF) [24]. In contrast, increased VEGF expression is a potent mitogen and permogen that increases in plasma and decreases in alveolar space in respiratory diseases. It is also known that an increase in VEGF causes an increase in lung damage [25]. In this study, it was shown by genetic analysis that the level of VEGF in the lung tissue of the 12-RAD group increased. Based on this result, we can say that radiotherapy contributes negatively to lung damage by causing an increase in VEGF level. ATX treatment, on the other hand, reduced the abnormally increased VEGF levels with radiotherapy and regressed the damage in the lung tissue. Oxidative stress and inflammation are closely linked. One of the most important sources of damage caused by inflammation is free oxygen radicals. Oxidative stress causes cells such as leukocytes to accumulate significantly in the lung tissue, causing inflammation [26-27]. In this study, decreases in TAS levels were found in the injury group treated with 12-RAD. From this point of view, in the case of 12-RAD, a lot of antioxidant use was needed to cope with oxidative stress. Accordingly, 12-RAD group had the lowest level. On the other hand, the significant increase in TOS and OSI levels in the 12-RAD group indicates that the increase in oxidant levels in case of damage causes oxidative stress. Reversing these negative outcomes in ATX treatment; reveals that ATX has antioxidant properties.

The activation of pathways that cause cellular stress results in radiation-induced cell death. Depending on the type of irradiation program and the dose used, stress occurs in the cell, and the existing balances in the cell are disrupted. This results in cellular death [5]. Apoptosis has an important place in various disease states and is regulated in various ways [28]. Excessive or insufficient apoptosis is associated with the pathogenesis of various diseases. Apoptosis is initiated by internal and external stimuli. External stimuli of apoptosis; activation of death ligands, exposure to ultraviolet, γ radiation; internal stimuli; DNA damage, oxidants, and increase in Ca2+ level can be given as examples [29]. Triggering apoptosis leads to both degradation of the protein substrate and cell death. Cas are proteins whose activities are heavily regulated, as inappropriate activation can have devastating effects [30]. Apoptotic cas is in an inactive form in the cell. Following activation of the apoptotic cascade, the initiator cas cleaves and activates the executioner cas-3, 6 or 7. Pro-cas-3 becomes an active enzyme when the two cleaved monomers combine to form an active dimer. This enzyme initiates the disintegration of the cell by disrupting the cellular architecture [31]. The data we obtained from the histopathological results show that cas-3 levels increased in the 12-RAD group. As a result, 12-RAD drives the cell to apoptosis by increasing cas-3 levels. Cas-3 levels decreased in the 12-RAD+ATX group. Based on these data, it can be said that ATX regresses apoptosis by causing a decrease in cas-3 levels. In other words, we can conclude that ATX significantly regresses lung tissue damage by showing anti-apoptotic activity.

In our study, we showed with our analysis that ATX regresses the lung damage caused by 12-RAD. Our results proved the efficacy of ATX in our study. The damage caused by 12-RAD was significantly reduced by ATX, showing anti-inflammatory, antioxidant, and antiapoptotic effects. All the evidence has shown that the use of ATX can be a potential treatment for radiotherapy-induced lung injury.

Conclusion

In our study, we showed with our analysis that ATX regresses the lung damage caused by 12-RAD. Our results proved the effectiveness of ATX in our study. The damage caused by 12-RAD was significantly reduced by ATX by showing anti-inflammatory, antioxidant, and antiapoptotic effects. All the evidences indicated that ATX usage could be a potential therapy to against radiotherapy-induced lung injury.

Statements & declarations

Funding

This study was supported by the Scientific Research Projects Coordination Unit of Suleyman Demirel University with project code TSG-2020-8134.

Competing interests

The authors have no relevant financial or non-financial interests to disclose.

Authors' contrubutions

Study was designed by Nursel Hasseyid, Suleyman Emre Akin, and Halil Asci. Material preparation, data collection, and analysis were performed by Yalcin Erzurumlu, Halil Ibrahim Buyukbayram, Hasan Ekrem Camas, Nursel Hasseyid, and Ozlem Ozmen. The manuscript was written by Nursel Hasseyid and Suleyman Emre Akin and edited by Halil Ascı. All authors read and approved the final manuscript.

Ethical approval

The animal experiments were approved by the local animal ethics committee of Suleyman Demirel University (Ethic No: 07.01.2021/01-05). This study has been carried out in accordance with the standards set out in the Code of Ethics of the World Medical Association (Declaration of Helsinki).

Conflict of interest

The authors declare that there is no conflict of interest.

Acknowledgments

Not applicable

Consent for publication

Not applicable

Availability of data and materials

All data generated or analyzed during this study are included in this published article.

References

1. Baskar R, Lee KA, Yeo R, et al. Cancer and radiation therapy: current advances and future directions. Int J Med Sci 9 (2012): 193-199.
2. Valentini V, Boldrini L, Mariani S, et al. Role of radiation oncology in modern multidisciplinary cancer treatment. Mol Oncol 14 (2020): 1431-1441.
3. Leal NF, Oliveira HF, Carrara HH. Supervised physical therapy in women treated with radiotherapy for breast cancer. Rev Lat Am Enfermagem 24 (2016): e2755.
4. Almeida C, Nagarajan D, Tian J, et al. The role of alveolar epithelium in radiation-induced lung injury. PLoS One 8 (2013): e53628.
5. Carvalho HA, Villar RC. Radiotherapy and immune response: the systemic effects of a local treatment. Clinics (Sao Paulo) 73 (2018): e557s.
6. Li MY, Liu JQ, Chen DP, et al. Radiotherapy induces cell cycle arrest and cell apoptosis in nasopharyngeal carcinoma via the ATM and Smad pathways. Cancer Biol Ther 18 (2017): 681-693.
7. Xu X, Lai Y, Hua ZC. Apoptosis and apoptotic body: disease message and therapeutic target potentials. Biosci Rep 39 (2019): BSR20180992.
8. Westhoff MA, Brühl O, Nonnenmacher L, et al. Killing me softly--future challenges in apoptosis research. Int J Mol Sci 15 (2014): 3746-3767.
9. Brotosudarmo THP, Limantara L, Setiyono E, et al. Structures of Astaxanthin and Their Consequences for Therapeutic Application. Int J Food Sci (2020): 2156582.
10. Kishimoto Y, Yoshida H, Kondo K. Potential Anti-Atherosclerotic Properties of Astaxanthin. Mar Drugs 14 (2016): 35.
11. Lowry OH, Rosebrough NJ, Farr AL, et al. Protein measurement with the folin phenol reagent. J Biol Chem 193 (1951): 265-275.
12. Erel O. A novel automated direct measurement method for total antioxidant capacity using a new generation, more stable ABTS radical cation. Clin Biochem 37 (2004): 277-285.
13. Erel O. A new automated colorimetric method for measuring total oxidant status. Clin Biochem 38 (2005): 1103-1111.
14. İlhan İ, Aşçi H, Hasseyid N, et al. Irbesartan decreased mitochondrial stress-related apoptosis in cisplatin induced acute kidney injury via regulating BCL-2/BAX signaling. Mol Biol Rep 49 (2022): 6125-6133.
15. Straub JM, New J, Hamilton CD, et al. Radiation-induced fibrosis: mechanisms and implications for therapy. J Cancer Res Clin Oncol 141 (2015): 1985-1994.
16. Arulselvan P, Fard MT, Tan WS, et al. Role of Antioxidants and Natural Products in Inflammation. Oxid Med Cell Longev (2016): 5276130.
17. Medzhitov R. Inflammation: new adventures of an old flame. Cell 140 (2010): 771-776.
18. Li Y, Huang X, Guo F, et al. TRIM65 E3 ligase targets VCAM-1 degradation to limit LPS-induced lung inflammation. J Mol Cell Biol 12 (2020): 190-201.
19. Sun CY, Zhao YX, Zhong W, et al. The expression of aquaporins 1 and 5 in rat lung after thoracic irradiation. J Radiat Res 55 (2014): 683-689.
20. Verkman AS, Mitra AK. Structure and function of aquaporin water channels. Am J Physiol Renal Physiol 278 (2000): F13-28.

21. Wittekindt OH, Dietl P. Aquaporins in the lung. Pflugers Arch 471 (2019): 519-532.

22. Tan J, Gao C, Wang C, et al. Expression of Aquaporin-1 and Aquaporin-5 in a Rat Model of High-Altitude Pulmonary Edema and the Effect of Hyperbaric Oxygen Exposure. Dose Response 18(2020): 1559325820970821.

23. Wang H, Hao X, Zhang L, et al. Decreased Expression of Aquaporin-1 in Lung Tissue of Silicotic Rats. Clin Lab 61 (2015): 1163-1169.

24. Hu K, Olsen BR. The roles of vascular endothelial growth factor in bone repair and regeneration. Bone 91 (2016): 30-38.

25. Varet J, Douglas SK, Gilmartin L, et al. VEGF in the lung: a role for novel isoforms. Am J Physiol Lung Cell Mol Physiol 298 (2010): L768-774.

26. WuG,DaiX,LiX,etal.AntıoxıdantAndAntı-Inflammatory Effects Of Rhamnazın On Lıpopolysaccharıde-Induced Acute Lung Injury And Inflammatıon In Rats. Afr J Tradit Complement Altern Med 14 (2017): 201-212.

27. Parlar A, Arslan SO, Doğan MF, et al. The exogenous administration of CB2 specific agonist, GW405833, inhibits inflammation by reducing cytokine production and oxidative stress. Exp Ther Med 16 (2018): 4900-4908.

28. Li J, Chen Q, He X, et al. Dexmedetomidine attenuates lung apoptosis induced by renal ischemia-reperfusion injury through α2AR/PI3K/Akt pathway. J Transl Med 16 (2018): 78.

29. Chambers E, Rounds S, Lu Q. Pulmonary Endothelial Cell Apoptosis in Emphysema and Acute Lung Injury. Adv Anat Embryol Cell Biol 228 (2018): 63-86.

30. Beroske L, Van den Wyngaert T, Stroobants S, et al. Molecular Imaging of Apoptosis: The Case of Caspase-3 Radiotracers. Int J Mol Sci 22 (2021): 3948.

31. Wall DM, McCormick BA. Bacterial secreted effectors and caspase-3 interactions. Cell Microbiol 16 (2014):1746-1756.